

Complexity and challenges in noncontact high temperature measurements in microwave-assisted catalytic reactors

Gangurde, Lalit S.; Sturm, Guido S.J.; Devadiga, Tushar J.; Stankiewicz, Andrzej I.; Stefanidis, Georgios D.

DOI

[10.1021/acs.iecr.7b02091](https://doi.org/10.1021/acs.iecr.7b02091)

Publication date

2017

Document Version

Final published version

Published in

Industrial and Engineering Chemistry Research

Citation (APA)

Gangurde, L. S., Sturm, G. S. J., Devadiga, T. J., Stankiewicz, A. I., & Stefanidis, G. D. (2017). Complexity and challenges in noncontact high temperature measurements in microwave-assisted catalytic reactors. *Industrial and Engineering Chemistry Research*, 56(45), 13379-13391. <https://doi.org/10.1021/acs.iecr.7b02091>

Important note

To cite this publication, please use the final published version (if applicable). Please check the document version above.

Copyright

Other than for strictly personal use, it is not permitted to download, forward or distribute the text or part of it, without the consent of the author(s) and/or copyright holder(s), unless the work is under an open content license such as Creative Commons.

Takedown policy

Please contact us and provide details if you believe this document breaches copyrights. We will remove access to the work immediately and investigate your claim.

Complexity and Challenges in Noncontact High Temperature Measurements in Microwave-Assisted Catalytic Reactors

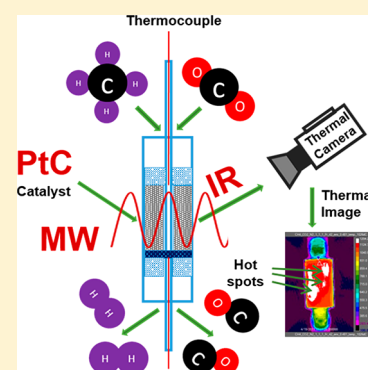
Lalit S. Gangurde,[†] Guido S. J. Sturm,[†] Tushar J. Devadiga,[†] Andrzej I. Stankiewicz,^{*,†,‡,ID} and Georgios D. Stefanidis^{*,†,‡,ID}

[†]Delft University of Technology, Process and Energy Department, Intensified Reaction and Separation Systems, Leeghwaterstraat 39, 2628 CB, Delft, The Netherlands

[‡]Katholieke Universiteit Leuven, Chemical Engineering Department, Celestijnenlaan 200F, 3001 Leuven, Belgium

S Supporting Information

ABSTRACT: The complexity and challenges in noncontact temperature measurements inside microwave-heated catalytic reactors are presented in this paper. A custom-designed microwave cavity has been used to focus the microwave field on the catalyst and enable monitoring of the temperature field in 2D. A methodology to study the temperature distribution in the catalytic bed by using a thermal camera in combination with a thermocouple for a heterogeneous catalytic reaction (methane dry reforming) under microwave heating has been demonstrated. The effects of various variables that affect the accuracy of temperature recordings are discussed in detail. The necessity of having at least one contact sensor, such as a thermocouple, or some other microwave transparent sensor, is recommended to keep track of the temperature changes occurring in the catalytic bed during the reaction under microwave heating.



1. INTRODUCTION

The history of microwave (MW) technology confirms its rapid development after the thermal effects of microwave heating were discovered in the 1940s.^{1,2} Since then microwave heating has been applied to food processing, polymer processing, plasma processing, organic chemistry, sintering of metals, inorganic material synthesis, and various industrial and research applications. Microwave heating in catalytic material synthesis, multiphase catalysis like gas–solid and solid–liquid reactions, has shown performance improvements as compared to the conventional heating mode, due to its rapid, selective, and volumetric nature.^{3–5} Along with its thermal effects, non-thermal microwave effects have also been reported to be responsible for increased catalytic activities resulting in overall improved process performance.⁵ In some works, energy consumption measurements of microwave heated processes have shown that lower energy consumption and higher heating rates are obtained compared to conventionally heated processes.^{6,7} Recent developments in wind, solar, plasma, and microwave technologies have shown the importance of microwave energy as a renewable, clean and exergetically efficient form of energy.^{8,9}

To use microwave energy efficiently for any chemical process requires a good understanding of process parameters and knowledge of materials response under their exposure to microwaves. Dielectric properties measurements provide insight into the heating ability of any material under microwave exposure.^{10,11} The dielectric properties of any material or fluid are described by their complex permittivity (ϵ^*). The complex

permittivity (ϵ^*) is divided into two parts: (a) the dielectric constant (ϵ'), or real part of the dielectric permittivity, represents the ability of the material to store electric energy in its structure; (b) the loss factor (ϵ''), or imaginary part of the dielectric permittivity, indicates the ability of the material to dissipate the stored electric energy in the form of heat. The ratio of the loss factor to the dielectric constant is called loss tangent ($\tan \delta$). Along with dielectric properties, the physics of electromagnetism involved during MW heating, the wave nature of microwave field, and its high degree of control are also essential to consider.¹² Therefore, it is important to know the dielectric properties of catalytic materials, preferably in the real reaction conditions, or at least in the expected temperature range of the catalytic application.

Horikoshi et al.¹³ reported generation of hot spots (electric discharges) and their impact on heterogeneous Suzuki–Miyaura coupling reaction for the synthesis of 4-methylbiphenyl in toluene solvent in the presence of Pd/AC catalyst. Zhang et al.¹⁴ studied microwave assisted sulfur dioxide reduction using methane over a MoS₂ catalyst and reported that the enhanced reaction performance was a result of hotspot generation within the catalyst itself. To generalize, nonuniform microwave and hot spots formation at particle or reactor scale

Special Issue: Tapio Salmi Festschrift

Received: May 22, 2017

Revised: September 6, 2017

Accepted: September 7, 2017

Published: September 7, 2017

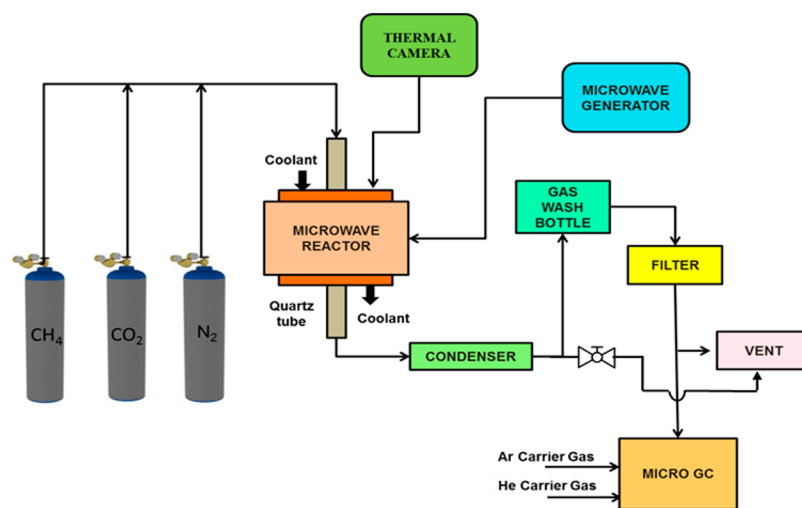


Figure 1. Schematic diagram of the microwave reactor setup.

frequently determine reactor performance. Hence, it is important to track these temperature patterns experimentally.

The major technical challenge for a detailed investigation of temperature distribution is the unsuitability of conventional methods and their limitations in measuring temperature under microwave heating. The tutorial review on temperature measurement in microwave-heated transformations, by Kappe,¹⁵ reports that accurate temperature measurement in a microwave heated system is a complex and nontrivial affair. The review is concerned with external temperature measurements and reports that surface measurements will always be problematic and will not adequately record temperature variations inside the reactor, although proper calibration for noncontact methods might provide realistic approximate temperature values. In earlier work from our group,^{16,17} fiber optic sensors were used to record temperature nonuniformities in solid catalytic beds in the axial and radial directions. Significant temperature gradients were found in a small amount of the sample heated in a monomode cavity. Recently, in the Ramírez group,^{18,19} a dual temperature measurement method of thermography combined with optical fiber was developed to investigate gas–solid temperature differences in a low-temperature range (100 to 250 °C), under microwave heating. In this method, the importance of corrected emissivity values to get accurate thermographic temperature readings from a thermal camera was demonstrated. These findings, however, were obtained in the low-temperature range (0 to 300 °C), where common optical fibers can be used. As optical fibers cannot be used above 300 °C, reliable temperature measurements under microwave heating above 300 °C become a major technical challenge to resolve.

A literature study reveals confusion regarding the direct use of metallic thermocouples in microwave reactions. Pert et al.²⁰ reported that the presence of thermocouples in microwave reactors can locally distort the electromagnetic field, induce thermal instabilities, and lead to serious measurement errors. Will et al.²¹ quickly inserted a thermocouple inside the catalytic bed when MW was turned off, to avoid thermocouple–microwave interaction resulting in sparks. In contrast, Li et al.²² directly used a thermocouple under microwave heating for methane mixed reforming. They reported that the interaction of the thermocouple with microwaves could be avoided by placing it in a 1-mm-thick quartz tube. Quartz, however, would

theoretically not be expected to shield a microwave field in this case, since its relative permittivity is $3.78-0.001i$, which is not nearly sufficient to attenuate a microwave field over a 1 mm distance.

Overall, direct use of a thermocouple inside a microwave reactor is risky, but its placement at the position where it would not come in contact with microwaves is a better experimental approach. Nonetheless, detection of hot spots and measurement of thermal gradients inside catalytic reactors are difficult with this approach. Previous simulation studies done in our group²³ show that local geometric and/or operating parameter variation at one point affects the microwave field over the entire volume in a microwave coupled system. Temperature measurement at one point inside the reactor is insufficient in heterogeneous catalytic processes.¹⁶ Therefore, an approach for simultaneous temperature measurements inside a reactor and on the reactor wall needs to be developed for high temperature microwave-heated reactors.

The aim in this work is to develop such an approach for heterogeneous catalytic reactions occurring under microwave heating in the range 300 to 1000 °C. The methane dry reforming ($\text{CH}_4 + \text{CO}_2 \leftrightarrow 2\text{H}_2 + 2\text{CO}$) reaction is taken as an illustrative example to study temperature distribution in the catalytic bed under microwave heating. First, dielectric properties of 10 wt % loading of platinum on activated carbon support (PtC) from room temperature to 850 °C are measured. A tailored microwave cavity has been constructed and used to focus the microwave field on the loaded reactor and collect thermal data in a 2D fashion. The factors affecting the thermal measurements are explained and demonstrated by means of an approach combining the use of a thermal camera and simultaneous thermocouple measurements. The existence of hot spots and their dislocations due to different gas environments under MW heating are shown. Thermal gradient differences in axial and radial positions in the catalytic bed are explained using thermal data post processing.

2. EXPERIMENTAL SECTION

2.1. Schematic Diagram of Microwave Reactor. A schematic diagram of the microwave reactor system is shown in Figure 1. The most important parts of this schematic are the custom-designed microwave reactor and quartz tube for the catalyst loading. The LabVIEW interface along with an NI-9074

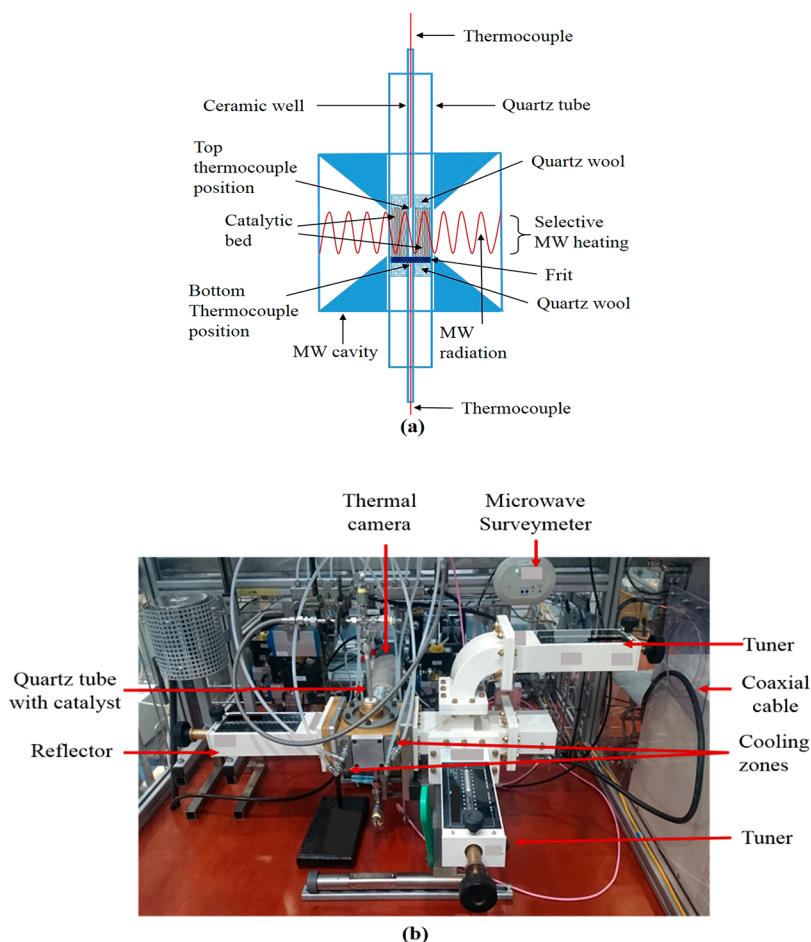


Figure 2. (a) Schematic diagram of catalyst and thermocouple positions in the quartz tube. (b) Digital image of the custom-designed MW reactor with a quartz tube inside.

cRIO controller is used to control the setup operation and perform data acquisition. The controller interfaces with valve status readouts, mass-flow controllers (Bronkhorst) to regulate gas flows, a pressure sensor, and N-type thermocouples. For noncontact temperature measurements, the thermal camera model FLIR A655sc is used. It operates in the 7.5–14 μm spectral range and measures temperatures from -40 to 2000 $^{\circ}\text{C}$. Thermal data from the experiments are collected via a PC using the FLIR ResearchIR Max software. A solid-state microwave generator (SAIREM Miniflow 200 SS) is used to supply the MW energy at 2.45 GHz. The maximum available power is 200 W.

A condenser is added at the exit of the reactor to avoid condensation in the ventilation line and the line toward the GC. Two thermostats are used to pump the coolant as a mixture of ethylene glycol and water at a ratio of 2:1 (EG/ H_2O). One is used to maintain the gas wash bottle temperature at -8 $^{\circ}\text{C}$. The second one maintains the MW cavity and condenser temperature at $+8$ $^{\circ}\text{C}$. The gas wash bottle is filled with CaO, as an adsorption agent, to dewater the remaining moisture in the outlet gas line. A Whatman FP050/1 filter holder with 50 mm filter paper and a Genie membrane are placed after the gas wash bottle to avoid any impurities toward the chromatogram. A Varian CP4900 micro-GC is used for product gas analysis. It is equipped with a TCD detector. It uses two columns, 20 m MS5A and 10 m PPU, for analysis. The LabVIEW interface, the μGC software, and the thermal camera

software were controlled by separate computers connected to one screen using a KVM switch.

2.2. Custom Designed Microwave Cavity and Other Equipment Used. For this work, as shown in Figure 2a and b, a custom-designed microwave cavity along with a catalyst loaded quartz tube has been used. The purpose of this new cavity is to (1) focus the electromagnetic field on the catalytic bed and (2) measure temperature with a thermal camera, so that more data can be gathered on the outer surface of a tube, in a 2D fashion, compared to temperature measurement at a single position. A germanium window (50 mm diameter \times 2 mm thick, 8–12 μm range) is installed inside the microwave cavity.

A quartz tube with a length of 290 mm, 1 mm wall thickness, 10 mm outer diameter, and 8 mm internal diameter was used for all heating and reaction experiments. Neoptix optical fibers (-80 to 250 $^{\circ}\text{C}$) were used for low temperature (<150 $^{\circ}\text{C}$) calibration and for verification of the temperature distribution from the center to the inner wall of the catalytic reactor up to 150 $^{\circ}\text{C}$, as thermocouples cannot be inserted inside the catalytic bed under microwave exposure. Two N-type thermocouples (-200 to $+1250$ $^{\circ}\text{C}$) with 0.5 mm diameter were used for high temperature measurements. Specifically, the thermocouples were placed at the top and bottom part of the catalytic bed (Figure 2a) to avoid MW–thermocouple interaction during MW heating.

2.3. Thermal Camera Working Principle. The main advantages of noncontact infrared thermal cameras are their speed and their ability to measure in broad temperature ranges. As a noncontact measurement technique, the thermal camera detector does not measure temperature directly; it calculates temperature using the Stefan–Boltzmann law and the emissivity value of the object or area of interest. The emissivity (ϵ) is a measure of an object's ability to emit infrared radiation. Eq 1 describes the relation between irradiation flux, temperature, and emissivity value¹⁸

$$J = \epsilon\sigma T^4 \quad (1)$$

where J is the irradiance flux, ϵ is the emissivity, and σ is Stefan–Boltzmann constant ($5.6 \times 10^{-8} \text{ m}^{-2} \text{ K}^{-4}$).

The emissivity change with temperature is a primary source of error in temperature measurements.²⁴ The emissivity also gets affected by structural or physical changes in the materials.²⁵ Inaccurate estimation of emissivity using table values incorrectly can also result in significant temperature measurement errors.²⁶ The emissivity of quartz glass has been reported to decrease with increasing temperature,²⁷ and the emissivity of metals or metallic powders increases parabolically with temperature.²⁴ The extraction of accurate temperatures using a thermal camera is not possible without corrected emissivity of the heated load.²⁶

In our case, the heated load (catalytic reactor) is a combination of Pt, carbon, and quartz tube of 1 mm thickness. As shown in Figure 3, the infrared radiation of the catalytic bed

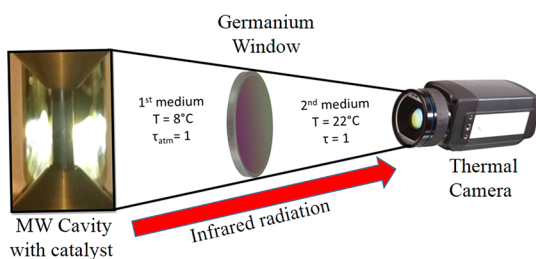


Figure 3. Schematic representation of the different media affecting the irradiance flux before reaching the thermal camera (where T is the temperature and τ is the transmittance).

has to travel through different mediums and through the germanium window from the microwave cavity to the camera detector. Therefore, it is imperative to consider medium changes during the emissivity calculation procedure to ensure its correct value. Overall, in our case, infrared radiation received by the thermal camera gets affected by (1) the microwave field distribution in the catalyst bed, (2) changes in transmittance of the quartz tube, (3) the microwave cavity wall temperature (8 °C) as a first medium, (4) the antireflected coated germanium window, and (5) the conditions of external atmospherics (22 °C), as a second medium. As the cavity wall to quartz tube distance is ~ 70 mm, the average temperature inside the cavity during microwave heating is expected to be higher than its wall temperature (8 °C) even with the application of cooling. However, in our case, the actual target temperature, as measured by the inside thermocouple, is provided to the camera software, which then automatically adjusts the apparent emissivity value according to the actual temperature given; therefore, the apparent emissivity value calculated is not affected by the temperature gradient outside the reactor.

2.4. Catalyst Loading for Microwave Heating. Figure 2a shows a schematic diagram of catalyst and thermocouple positions in a quartz tube. Initially, ~ 1000 mg of powdered PtC catalyst was pressed at 20 kg/cm^2 to make a pellet. The pellet was broken again to make sieves in a size range of $75\text{--}112 \mu\text{m}$. The sieved powder was heated in an electric oven at 140 °C for 3 h to remove its moisture content. As shown in Figure 2a, first, a quartz wool plug was fixed in the quartz tube. Then, a quartz P3 frit (thickness 1.5 mm, diameter 7.9 mm, and pore size $40\text{--}60 \mu\text{m}$) was placed on top of it. The purpose of adding the frit is to keep the ceramic well (99.8% dense alumina, o.d. = 3 mm and i.d. = 2 mm) position at the center of the quartz tube. The ceramic well was used to protect the thermocouple and to prevent its interaction with the microwave field. As shown in Figure 2a, 500 mg of catalyst was loaded above the frit and equally distributed around the ceramic well. It was then tapped to maintain the bed compactness, and another quartz wool layer was added on the top to retain bed compactness. The reactor tube was then placed in the microwave cavity. The required thermocouple lengths to monitor the top and bottom positions of the catalytic bed were already measured and then inserted into the ceramic well to avoid microwave–thermocouple interaction.

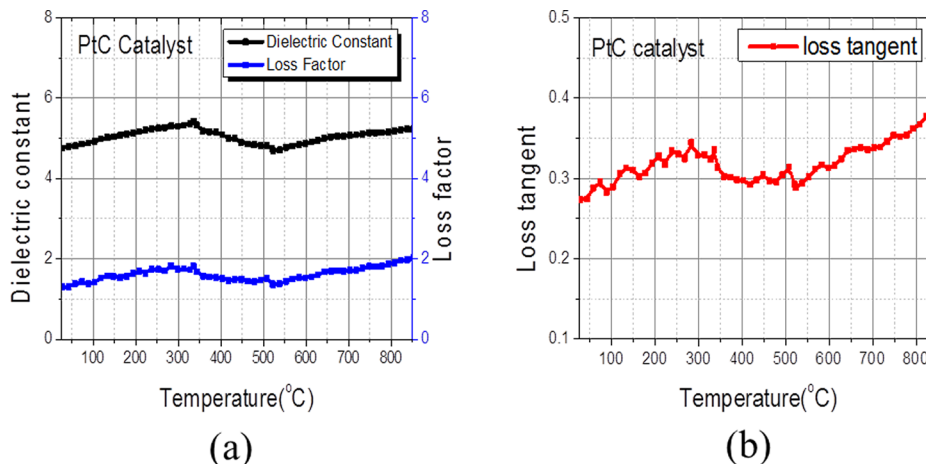


Figure 4. (a) Dielectric constant (ϵ') and loss factor (ϵ'') vs temperature. (b) Loss tangent (δ) vs temperature.

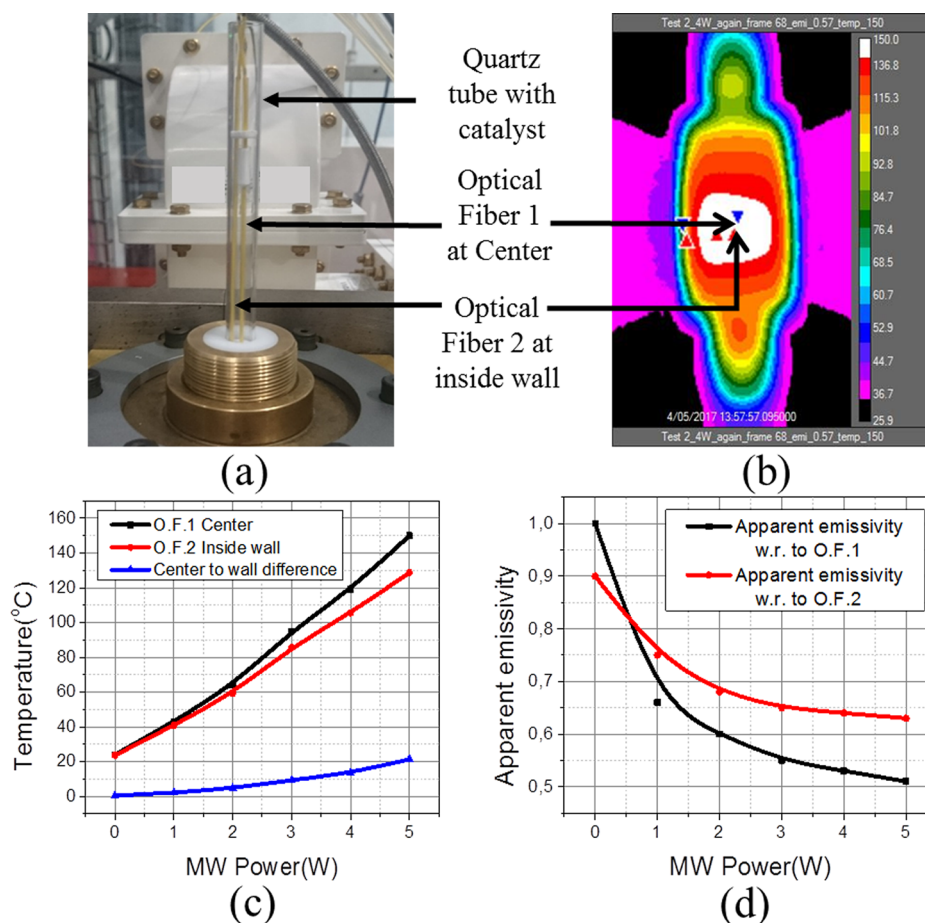


Figure 5. (a) Digital image of a quartz tube inserted in the MW cavity along with two optical fibers. (b) Thermal image showing the points where emissivity was calculated with reference to optical fibers. (c) Temperatures and temperature difference measured by the two optical fibers. (d) Emissivity calculated with reference to optical fibers' temperature.

2.5. Dry Reforming Reaction Testing Procedure under Microwave Heating.

It is difficult to control and provide MW energy when the selective heating behavior of a complex catalytic system is unknown. Hence, first, a MW heating test under real reaction conditions was performed by increasing power from 0 to 200 W. From this heating test and reaction performance evaluation, 150 W of MW power was found to give the maximum reactant conversions for the PtC catalyst used. Therefore, we performed methane dry reforming at 150 W, 34 mL/min total reactant gas flow at 1:1 volume ratio of CH_4/CO_2 , and atmospheric pressure. Once the catalyst reached a stable temperature under a N_2 flow with 150 W, methane and carbon dioxide reactant gases were fed to the reactor. After 1000 s of MW heating time, the product gases were repetitively analyzed by the chromatogram (GC) every 400 s of reaction time to evaluate the reaction progress.

3. RESULTS AND DISCUSSION

3.1. Dielectric Properties of Catalyst Measured at High Temperature.

Dielectric properties of 10 wt % platinum on carbon (PtC) were measured in specially designed equipment at the ITACA Institute of Valencia University, Spain. The methodologies mentioned in refs 28 and 29 have been followed for the measurements. The PtC sample was placed in a quartz tube, which was located inside the specially designed setup. The dielectric properties were measured while simultaneously the sample was heated at 20 °C/min under a N_2

atmosphere. The used methodology is based on the shift of the center resonant frequency and the alteration of the quality factor of the microwave cavity in the presence of PtC catalyst as compared to the empty cavity. The measurements were done in the range 20–850 °C. The accuracy of dielectric measurements was estimated as 3% for the dielectric constant and 10% for the loss factor in the entire measured range.

Three cycles of heating up to 850 °C with a heating rate of 20 °C/min followed by natural cooling using 0.507 g of PtC catalyst were performed. The evolution of the dielectric properties of the catalyst with temperature in the third cycle is shown in Figure 4. Figure 4a and b show that the materials' dielectric properties have an overall increasing trend in the examined temperature range, but this trend is not monotonic.

The preprocessing or preheating of some materials may result in a change of their physical or chemical properties, e.g., density, which can also affect their dielectric properties. The observed decrease in the dielectric properties values at 360–375 °C is due to sample volume reduction as shown in Figure S2. This volume reduction could be attributed to moisture removal, and shrinking of the material occurred during the heating up to 850 °C. The possibility of sample reduction due to moisture removal was not expected to happen after the first measurement cycle, as the sample tube was not open to absorb water before the second and third cycles. Therefore, volume reduction in the second and third cycles was mostly due to shrinking of the sample, which is responsible for the density

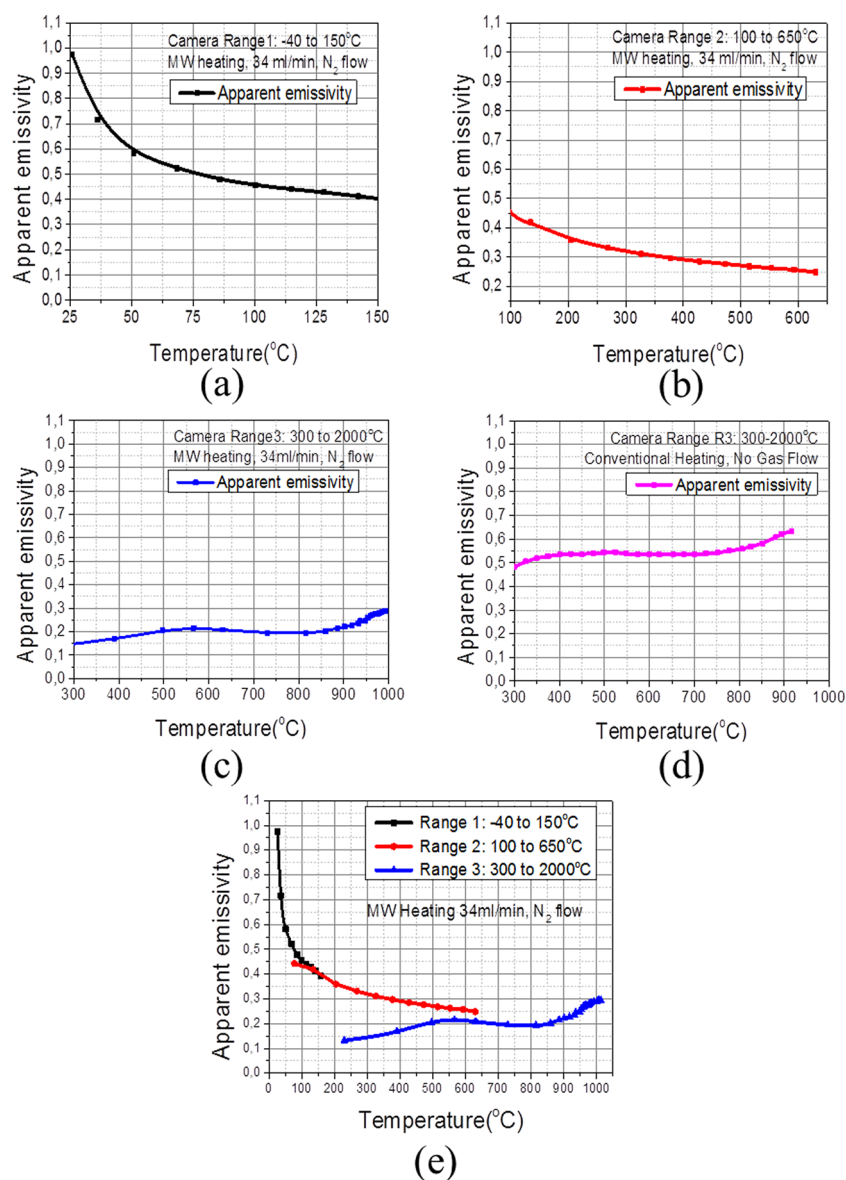


Figure 6. Effect of camera range and heating mode on emissivity. (a) First camera range (-40 to 150 °C), (b) second camera range (100 – 650 °C), (c) third camera range (300 – 2000 °C). (d) Emissivity calculated in conventional heating with the third camera range (300 – 2000 °C) and (e) three camera ranges together.

change of the material and hence of the dielectric properties in the temperature range 360 – 375 °C. However, the effect of platinum might be predominant at temperatures higher than 600 °C, which results in increasing dielectric property values at temperatures above 600 °C.

3.2. Radial Temperature and Emissivity Differences by Optical Fibers. As thermocouples cannot be inserted directly inside the microwave field, we performed low temperature heating tests using optical fibers to calculate emissivities at the center and inner wall optical fiber positions. Figure 5a shows the catalyst loaded quartz tube that is placed inside the microwave cavity along with two optical fibers kept in glass capillaries. The first sensor is placed at the center of the reactor and the second one at the inner wall of the quartz tube. Optical fiber 1 was directly connected to a microwave generator to limit the microwave heating in the workable temperature range of the optical fibers. Optical fiber 2 was connected to a

nomad touch optical thermometer to record its thermal response.

The catalytic bed was heated from 1 to 5 W of MW power without any gas flow as shown in Figure 5c. The thermal videos were recorded for 120 s with a recording rate of 1 frame per second after a stable temperature was achieved at the supplied power. The emissivity at the optical fiber positions at the inner side of the wall and at the center was calculated with an inbuilt calculator of camera software. The cursor of the 3×3 pixel was placed at the locations shown in the thermal image of Figure 5b. A quartz tube to camera distance of 0.3 m was considered along with actual temperature values to calculate the emissivity. Other settings, shown in Figure 3, for the first medium cavity environment (temperature 8 °C, 100% transmittance), second medium (air at temperature 22 °C, 100% transmittance), and germanium window (temperature of 22 °C, 96% transmittance) were also adjusted in the camera software aside from the calculation of emissivity.

As shown in the emissivity graphs of Figure 5c and d, the emissivity values at the center optical fiber 1 and at the inside wall optical fiber 2 can help obtain the direct center-to-inner surface temperature differences at the same quartz surface location. Figure 5d clearly shows a decreasing trend of emissivity with an increase in temperature in both the center and surface cases. The emissivity value at the center is observed to be lower than the inside wall emissivity as temperature increases. These low-temperature heating experiments showed that center temperature emissivity and inside wall emissivity are very helpful to finding the radial temperature differences. Figure 5c clearly shows that as the temperature inside the catalytic bed increases, the center-to-inner wall temperature difference also increases. The temperature measurement just at the surface of the catalytic bed will provide a lower temperature value than the actual center temperature value. Therefore, a thermal camera or any other IR measuring system should be directly calibrated with respect to a center temperature sensor, or a surface temperature sensor, to ensure the accuracy of the apparent emissivity at the respective point.

3.3. Effect of Camera Range and Heating System Used. The thermal camera has three different ranges to measure temperature. These temperature ranges have shown some influence on the emissivity calculations. Therefore, a separate heating experiment for each range was performed, and the emissivity was calculated accordingly. To ensure the accuracy of thermocouple temperature measurement, a heating test was done by placing a thermocouple and an optical fiber together at the top part of the catalytic bed. Heating was performed without N₂ gas flow. The temperatures shown by both sensors were very close to each other as shown in Table S2. This test also confirmed that microwaves do not interact with the thermocouple during heating. To study the effect of camera range, the catalytic material was microwave-heated in the temperature range 120–140 °C for 60 min under a N₂ flow of 34 mL/min to remove the moisture absorbed during the loading procedure. After this initial heating for 60 min, the MW generator was switched off, and the system was allowed to cool down to room temperature. Once the system reached a stable room temperature, temperature measurement with the thermocouple and thermal frame capturing were started, and recording was done every 120 s to collect data simultaneously after the MW was on until the end of the MW heating experiment. The MW generator was switched on with a power of 1 W increase per 120 s for the first (–40 to 150 °C) range of data collection and increased 5 W per 120 s for the second (100 to 650 °C) and third (300 to 2000 °C) ranges of data collection. During post processing of thermal data, the emissivity was calculated for each range with reference to the actual inside temperature shown by a thermocouple.

Figure 6 compares the effect of camera range on emissivity values in microwave heating. Figure 6a shows that in the first range of –40 to 150 °C, emissivity changes from 0.97 at 25 °C to 0.41 at 140 °C. Figure 6b shows that in the second range of 100 to 650 °C, emissivity decreases from 0.41 at 134 °C to 0.24 at 630 °C. In the third temperature range of 300 to 2000 °C, emissivity starts from a very low value of 0.16 at 390 °C and reaches a local maximum of ~0.22 at ~575 °C; then it remains at ~0.2 up to 850 °C and finally increases monotonically up to 0.29 at 1000 °C.

As thermal cameras are factory calibrated for particular ranges, it is imperative to use them in their specified ranges only. The selection of suitable camera range as per temperature

of interest, e.g., 600 to 1000 °C for dry reforming of methane, suggests that the third camera range is suitable. Therefore, while comparing experimental results, use of the same camera range can minimize the error due to different camera ranges as shown in Figure 6e in 300–600 °C common scale. Two different ranges have different color or scale bars, which again creates a problem for visual comparison. In addition, hot spots that may be occurring at higher temperatures than the maximum limit of the camera range, during MW heating, may form another reason for inaccuracies in temperature calculation.

Comparison of Figure 6b and c on a common temperature interval 300–650 °C shows a clear effect of the camera range on the emissivity and temperature values. For example, the emissivity values of 0.24 and 0.21 at 630 °C in the second (Figure 6b) and third (Figure 6c) range, respectively, show the clear effect of different camera range settings used on the temperature recordings. Specifically, if an emissivity value of 0.24 from the second range is used in the third temperature measurement range, then it matches with a thermocouple reading only at 948 °C. Therefore, use of a suitable thermal camera range for the required working temperature is necessary in order to have a fair comparison of heating patterns, or to study the influence of other parameters on temperature or heating patterns.

Another interesting aspect is the influence of the heating system on emissivity values. Figure 6d shows the graph of emissivity measurements done in conventional heating using the tubular furnace (digital image in Figure S1) without N₂ flow. In this heating experiment, a quartz tube, with the catalyst sandwiched between quartz wool plugs, along with a thermocouple at the center of the catalytic bed was placed in a tubular furnace. The loaded tube was heated up to 970 °C (the upper temperature limit of the furnace is 1000 °C). After getting stable temperature values, the thermocouple and thermal camera recording were started. The tube along with the thermocouple was pulled out from the bottom side of the furnace until the catalytic bed was visible to record the thermal video (see Figure S1). The quartz tube to thermal camera distance was also kept at 0.3 m in the conventional heating experiment. The emissivity values were calculated in the same manner as mentioned before from 300 to 900 °C.

It is clear in the case of conventional heating (Figure 6d) that emissivity varies with an increase in temperature and stays in the range from 0.48 to 0.63 for the 300–900 °C temperature range. In the case of microwave heating, it stays with its lower value of 0.16 to 0.22 only for the 300 to 900 °C range and shows a fast increasing trend up to 1000 °C, where it becomes 0.29. The increased value of emissivity obtained by the conventional heating system explains the reasons behind the decreased emissivity in the microwave heating system. The first reason is the N₂ flow that removes heat from the catalytic bed, and the second reason is the medium through which the irradiance has to pass to reach the thermal camera.

This comparative study has also suggested that if the emissivity calibration is done in conventional heating with different conditions and the values obtained are used for microwave heating experiments, then these values will be unable to provide accurate temperature values during microwave heating experiments. Therefore, in situ emissivity calculations under microwave heating are necessary for noncontact temperature measurement techniques using IR cameras.

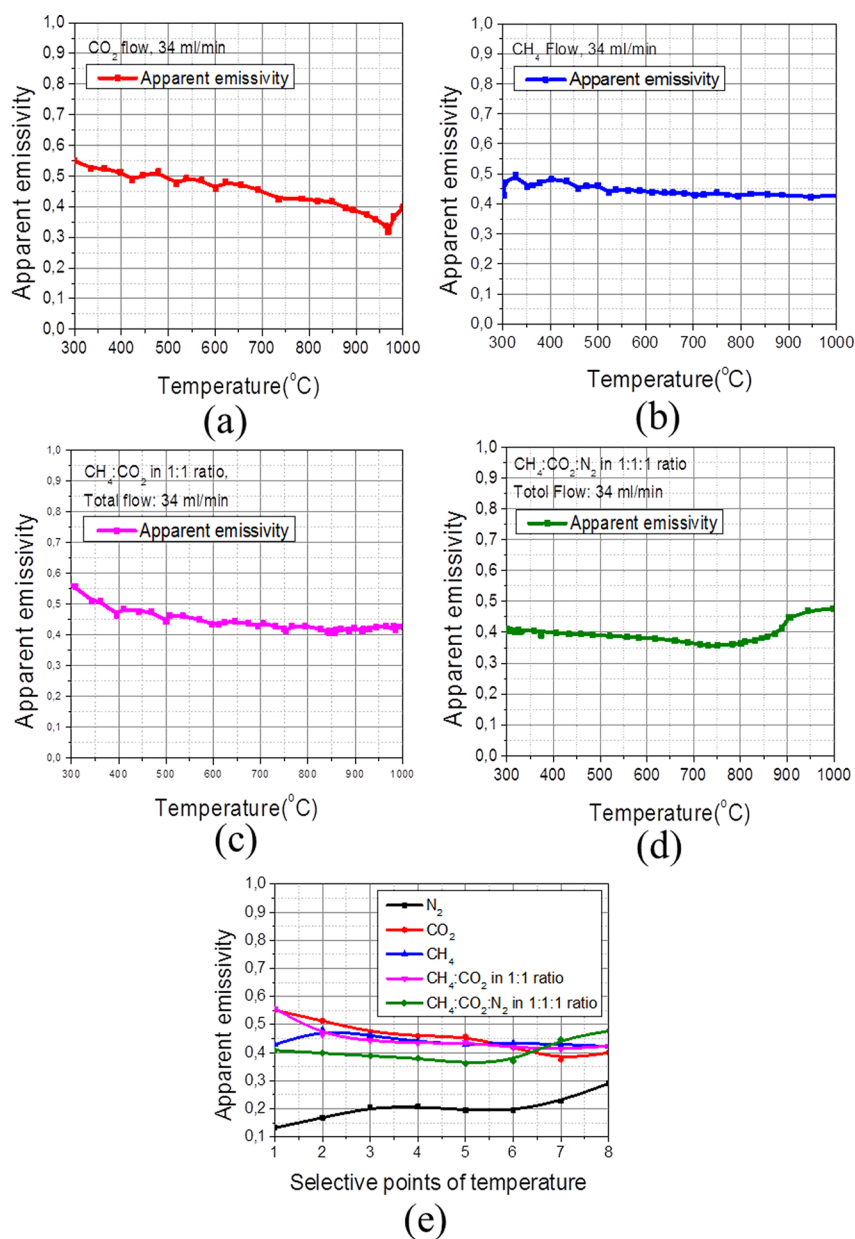


Figure 7. Effect of different gases on emissivity. (a) CO_2 , (b) CH_4 , (c) CH_4/CO_2 at 1:1 flow ratio, (d) $\text{CH}_4/\text{CO}_2/\text{N}_2$ in 1:1:1 flow ratio, and (e) comparison of emissivities under different gas flows (see Table S1).

3.4. Effect of Gases on Emissivity and Detection of Hot Spots. It has been reported that the presence of different gases and reactions in the catalytic material influences the emitted infrared radiation¹⁸ and eventually affects the apparent emissivity. Gases such as CO , CO_2 , CH_4 , H_2 , N_2 , and other hydrocarbons have significant absorption bands due to their vibrational and rotational motions in the infrared range. As methane dry reforming involves most of the gases mentioned above, the emissivity calculated in N_2 flow is not applicable to detecting the temperature changes occurring during the reaction. Therefore, we studied the influence of separate reactants and their possible combinations on emissivity under actual reaction conditions until 1000 °C.

Figure 7 shows the effect of different gas flows on emissivity values. Figure 7a shows the apparent emissivity in CO_2 gas flow. It shows that the emissivity value is 0.55 at 300 °C and gradually decreases with increasing temperature. Figure 7b

shows a lower emissivity value of 0.42 in CH_4 flow as compared to CO_2 flow at 300 °C. The emissivity under CH_4 flow shows some fluctuations up to 562 °C, and then it slightly decreases and remains at 0.42 up to 946 °C. Figure 7c shows the emissivity for a combination of CO_2 and CH_4 at a 1:1 ratio in total flow. Emissivity is 0.55 at 300 °C; then it decreases to 0.44 at 571 °C with some fluctuations and eventually reaches a seemingly plateau value of 0.42 at 1000 °C. Figure 7d shows the effect of the combination of $\text{CO}_2/\text{CH}_4/\text{N}_2$ flow, at a 1:1:1 ratio, on the emissivity. The emissivity in this case is 0.4 at 300 °C; it decreases gradually up to 0.35 around 731 °C and then increases up to 0.47 at 998 °C. Figure 7e shows a direct comparison of the emissivity calculated under different gas flows. As comparison at precise temperatures is not possible in our case, some selective points from each test are taken to show a direct comparison (values are given in Table S1). This comparison reveals that there are no big differences in the

apparent emissivities under CO₂ and CH₄ flow. However, the emissivity under CO₂ flow has higher values among all tested gases up to 690.35 °C. The decrease in the emissivity of CO₂ past 690.35 °C is due to the migration of hot spots in the catalytic bed. A continuous fluctuation in the apparent emissivities is observed due to the continuous migration of the hot spots during the experiments shown in Figure 7e. Aside from the different heat removal properties of different gases, another possible reason for the different emissivity values under pure and combined gas conditions could be the change in the total dielectric properties of the catalytic material due to pyrolytic carbon formation or direct structural changes in catalytic materials.

The different trends of the gas emissivity lines at high temperatures, past point 6 in Figure 7e, may be due to dissociation of reactant gases and formation of product gases, which would affect the resultant irradiation flux. This comparison confirms that using only N₂ flow values will provide inaccurate information on temperature changes inside the bed.

Along with finding emissivities for different gases, it is necessary to study 2D heat distribution in the catalytic bed in order to get insight into possible hotspot generation and nonuniform heating under MW exposure. The existence of hot spots in solid–liquid reactions has already been shown by high speed cameras.¹⁵ Studies done by Chen et al. for methane thermocatalytic decomposition showed that there was a 125 °C difference between the reactor inside and outside temperatures in microwave-heated heterogeneous catalytic systems.³⁰ Zhang et al. have also reported that hot-spot temperatures were found to be 100–200 °C higher than the temperatures measured by optical thermometer.³¹ Therefore, getting precise information on hot spot formation under microwave heating can support the discussion on possible factors determining process intensification. The thermal camera gives the advantage of finding out the exact locations of these hot spots in the catalytic bed, thanks to its rainbow pellet option to show hot spot positions inside the catalytic bed. Figure 8a and b show the loaded quartz tube along with the N₂ flow thermal image. This thermal image shows that, in the case of the N₂ flow test, the temperature is higher at the center of the catalytic bed. It also reveals that the temperature where the emissivity has been calculated is lower than the center temperature of the catalytic bed (see the scale bar of the thermal image in Figure 8b). The camera does not only provide a range of hot zones but also gives the highest temperature point present in the catalytic bed which is 1151 °C under a N₂ flow.

The thermal images shown in Figure 8 confirm the presence of hot spots or zones and their shift or dislocation inside the catalytic bed with different gas flows. In addition, the thermal images in Figure 8 can explain the fluctuations of emissivity values observed under different gas flows. It is clear in the thermal images that hot spots can migrate or split with respect to different gases present in the bed and with the duration of heating. Indeed hotspot locations change during MW heating due to the interaction of these gases with the catalyst, or homo-heterogeneous reactions.

The live streaming and recording option of the thermal camera allows for monitoring, in real time, changes in the heating patterns inside the catalytic bed. In most of the literature on heterogeneous catalysis in the temperature range 700–1000 °C under microwave heating, clear evidence on temperature differences between hot spots and average

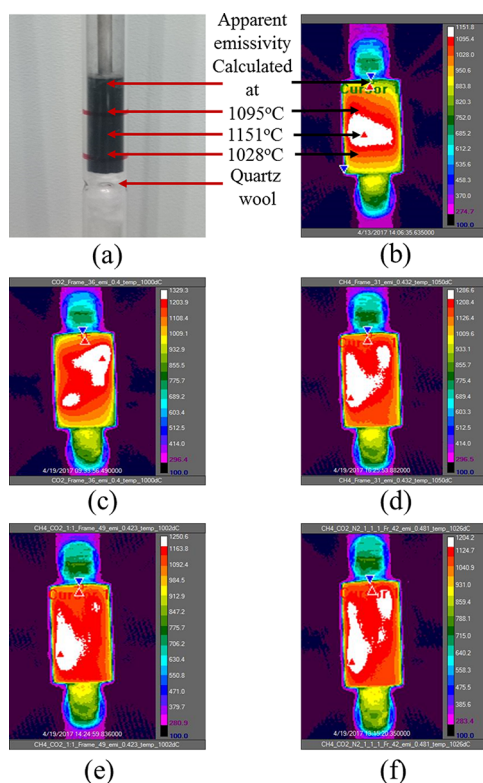
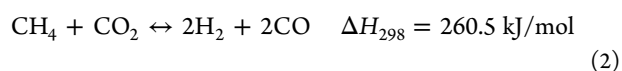


Figure 8. (a) Catalyst loaded quartz tube and detection of hot spots in the catalytic bed under different gas flows shown by thermal images in (b) N₂, (c) CO₂, (d) CH₄, (e) CH₄/CO₂ at a 1:1 ratio, and (f) CH₄/CO₂/N₂ in 1:1:1 ratio.

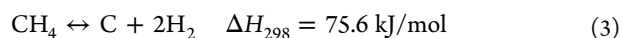
temperature is missing. This dual approach of matching internal and external temperature values with the help of a thermal camera provides the most accurate values for temperature differences.

3.5. Catalyst Performance Evaluation and Microwave Absorption Efficiency. The dry reforming of methane is a highly endothermic reaction (reaction 2). It involves a combination of the two reactions mentioned below: catalytic CH₄ decomposition (reaction 3) and CO₂ gasification (reaction 4).³²

Dry reforming



Methane decomposition



Carbon dioxide gasification

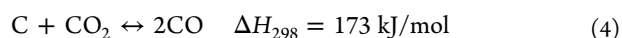


Figure 9a shows CH₄ and CO₂ conversion over the PtC catalyst with 150 W of microwave power for 270 min of total reaction run. The conversions of methane and carbon dioxide were calculated by using the following equations:

$$\begin{aligned} &\text{CH}_4 \text{ conversion, \%} \\ &= 100 \times \left[\frac{(\text{H}_2)_{\text{out}}}{2} \right] / \left[(\text{CH}_4)_{\text{out}} + \frac{(\text{H}_2)_{\text{out}}}{2} \right] \end{aligned} \quad (5)$$

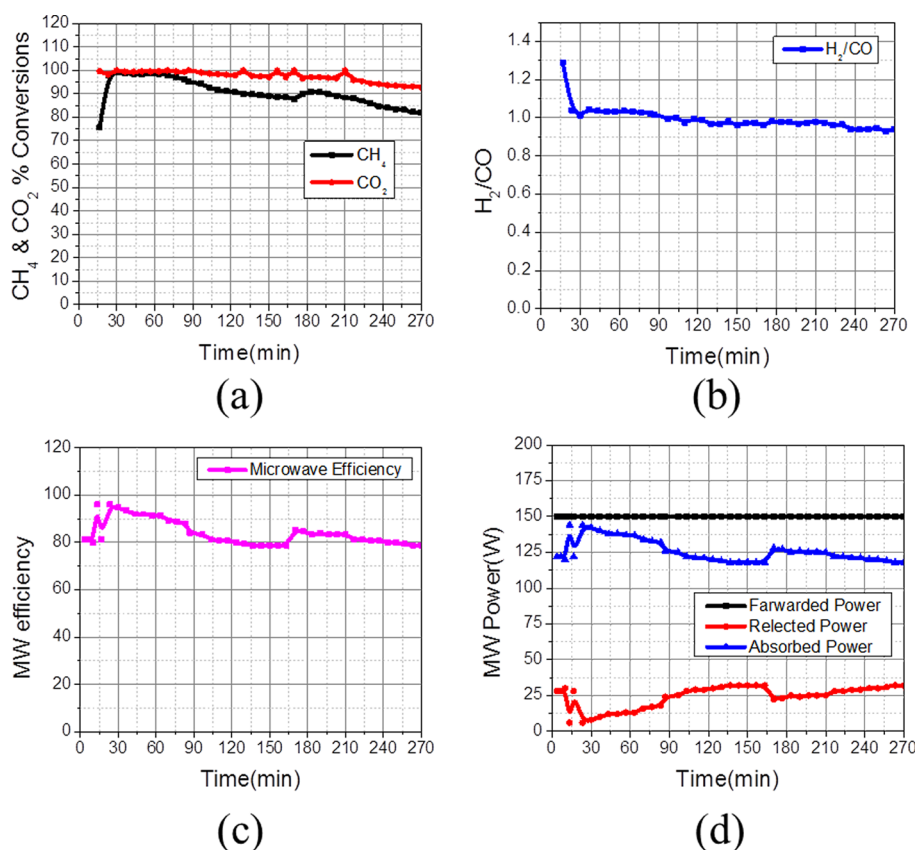


Figure 9. Methane dry reforming results. Temporal profiles of (a) CH₄ and CO₂ conversion; (b) H₂/CO ratio; (c) microwave energy absorption efficiency; and (d) forwarded, absorbed, and reflected microwave powers.

CO₂ conversion, %

$$= 100 \times \left[\frac{(\text{CO})_{\text{out}}}{2} \right] / \left[(\text{CO}_2)_{\text{out}} + \frac{(\text{CO})_{\text{out}}}{2} \right] \quad (6)$$

where (CH₄)_{out}, (H₂)_{out}, (CO₂)_{out}, and (CO)_{out} are methane, hydrogen, carbon dioxide, and carbon monoxide concentrations in the effluent gas (% by volume), as determined by gas chromatography. The microwave energy utilization efficiency was calculated by the following formula:

MW energy utilization efficiency

$$= \left[\frac{(\text{Forwarded Power (W)} - \text{Reflected Power (W)})}{\text{Forwarded Power (W)}} \times 100 \right] \quad (7)$$

The conversion graph in Figure 9a shows that CO₂ conversion is always higher than CH₄ conversion. As reaction time increases, CH₄ conversion decreases from 99% to 80% and CO₂ conversion decreases from 99% to 92%, while the H₂/CO ratio remains at ~1 (Figure 9b), during the complete run of 270 min. Zhang et al.³¹ have carried out dry reforming experiments and observed that, at temperatures higher than 700 °C, the heating efficiency was markedly reduced and a high power level was needed to increase temperature. This observation is qualitatively consistent with the lower MW power absorption and the reduction in MW energy efficiency with time in our case too. Figure 9c shows that the microwave absorption efficiency at 30 min is ~94%; it decreases to ~78%

after 270 min of reaction time. The main reason for the decrease in conversion with time is deactivation of the catalyst. As the reaction runs for a long time, the formation of a pyrolytic carbon layer becomes significant on the inside wall of the quartz tube. The graphitic character of this deposited layer is responsible for the increase in the reflected power and hence compromises the overall microwave absorption ability of the catalytic bed.³³ As less MW energy is getting absorbed by the catalytic bed, the temperature in the catalytic bed decreases and results in a decrease in conversion with time.

3.6. Emissivity Matching during the Reaction. Figure 10a shows the emissivity matching with thermocouple reading during the dry reforming process and its sensitivity to changes occurring in the catalytic system. First, the already calibrated emissivity value of 0.421 for a 1:1 ratio of CH₄/CO₂ was used. However, this emissivity was not matching with the actual temperature changes shown by the thermocouple. To get more realistic temperature values, we took actual temperature values shown by the thermocouple as a reference and recalculated the emissivity. After several trial-and-error attempts, a value of 0.737 was found to be the correct match for the stable temperature of ~800 °C in the time interval 100 to 166 min. At 166 min, due to a technical reason, the MW generator turned off, and then the reactor did not receive a MW supply for 30 s until the generator was restarted again. Once the MW was on again, we observed that the emissivity value was changed and decreased to 0.687, which was matching with the thermocouple temperature values. In continuous MW heating experiments, if the dielectric properties of the catalytic bed change due to physical or chemical properties changes in the catalytic bed

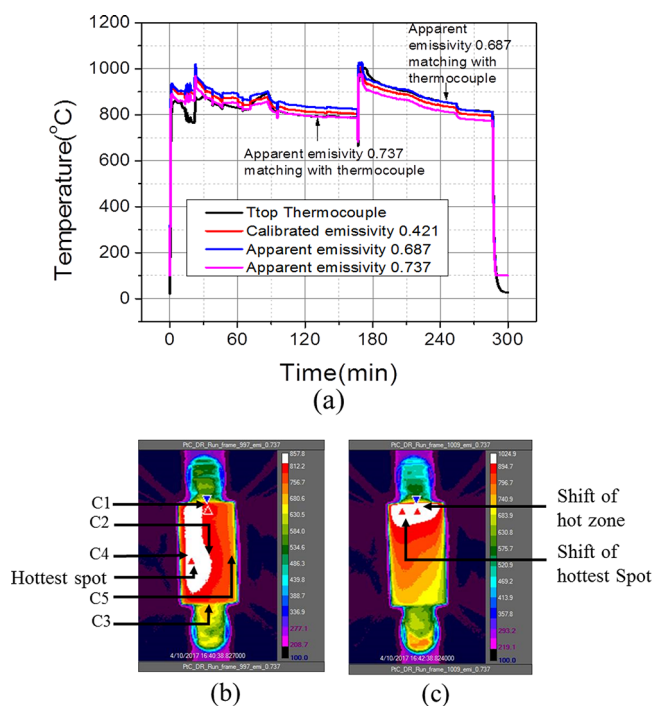


Figure 10. (a) Emissivity matching with actual temperature shown by a thermocouple during the methane dry reforming reaction. (b) The thermal image at 166 min; temperature values are extracted from the thermal video at C1 (top), C2 (center), C3 (bottom), C4 (left), and C5 (right) positions to study temperature distribution at these points. (c) The shift of hot spot or zone due to MW supply discontinuity.

itself (resulting from high processing temperatures), then migration or a shift of hot spots will also happen.

3.7. Factors Affecting the Emissivity and Overall Temperature Distribution during the Reaction. Figure 11a shows the graph of temperature profiles with factors affecting the emissivity and temperature fluctuations during the reaction. As the reaction proceeds and reactant gases get converted to product gases, fluctuations in the intensity of emitted irradiation occur. A thermocouple remains unaffected by these changes and becomes the reference for emissivity correction at any time during the reaction. In Figure 11a, the black line represents the temperature shown by the thermocouple. As it is not possible to change emissivity manually at every point, we selected the emissivity value of 0.737 after the emissivity match test reported earlier (see Figure 10a).

Figure 11a shows that after switching on the microwave generator, the catalyst reaches a temperature above 700 °C in 70 s under a N₂ gas flow. After 600 s, CH₄ and CO₂ were fed to the reactor at a flow rate of 17 mL/min for each gas. MW tuning was done to minimize the reflected power and to focus all forward power to the catalyst only. After reactant feeding, a decrease in temperature is observed (see black line in Figure 11a). This decrease in temperature could be due to an increase in the reflected power, which means that lower microwave energy is absorbed, and due to the endothermic nature of the reaction. As the reaction proceeds, more energy is utilized due to the endothermic nature of the reaction; this lowers the overall temperature of the catalytic bed and hence emits less infrared radiation that reaches the camera detector.

At 13, 16, and 23 min intervals, reflector tuning was done to maximize utilization of MW energy. Therefore, sudden high

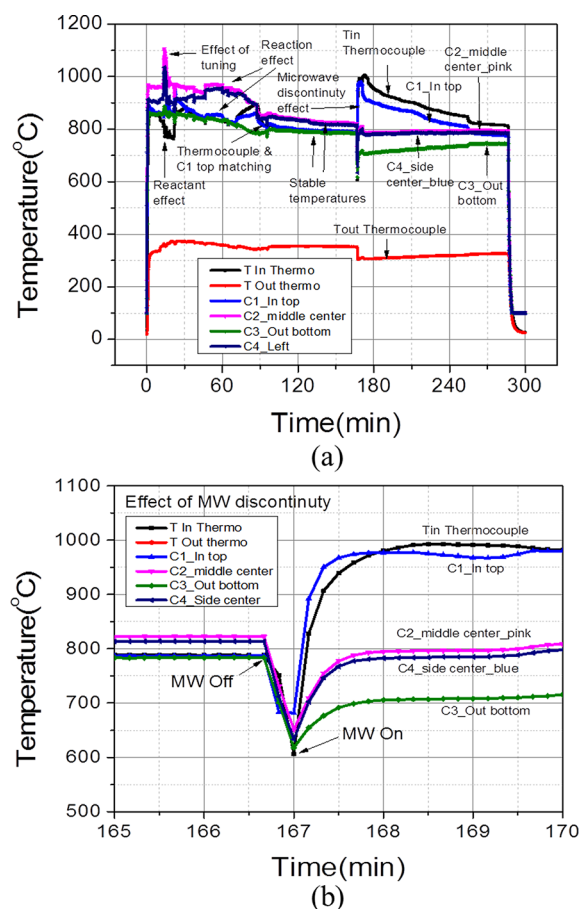


Figure 11. (a) Factors affecting temperature distribution in the catalytic bed during the reforming reaction. (b) Effect of MW supply discontinuity on emissivity and temperature distribution.

peaks at the surface temperatures are shown by the thermal camera values, but the thermocouple shows a decrease in temperature until 16 min (Figure 11a). This mismatch is a result of two things: (1) the change in infrared radiation occurring due to reaction progress and (2) the emissivity value used for this analysis is not applicable for these initial temperature changes.

A big drop in temperature from ~780 to 600 °C within 30 s was observed at ~166 min (Figure 11b). Once the MW was on again, a sudden increase in temperature was observed after this gap. This incident changed the emissivity after 166 min. The temperature profiles at top, middle, and bottom are separated after 166 min, but the temperature differences were observed to decrease until 270 min. In order to get a good match again with the temperature values shown by the thermocouple, a new emissivity was calculated with new thermocouple readings after 166 min. The reason for this change in temperature and emissivity values can be explained by the thermal images shown in Figure 10b and c. The shift of hot spot or zone from the left side of the catalytic bed (Figure 10b) to the top of the bed, where the thermocouple is placed (Figure 10c), clearly explains the sudden increase in temperature as the hot spot is very close to the thermocouple and the location where it is calculated. The physical reason behind the change in emissivity is the sudden increase in temperature or shift of hot spot in the catalytic bed. This increase in temperature happened because of two things: first, when the MW power was off, the temperature dropped from 780 to 600 °C, while reactant gases were still

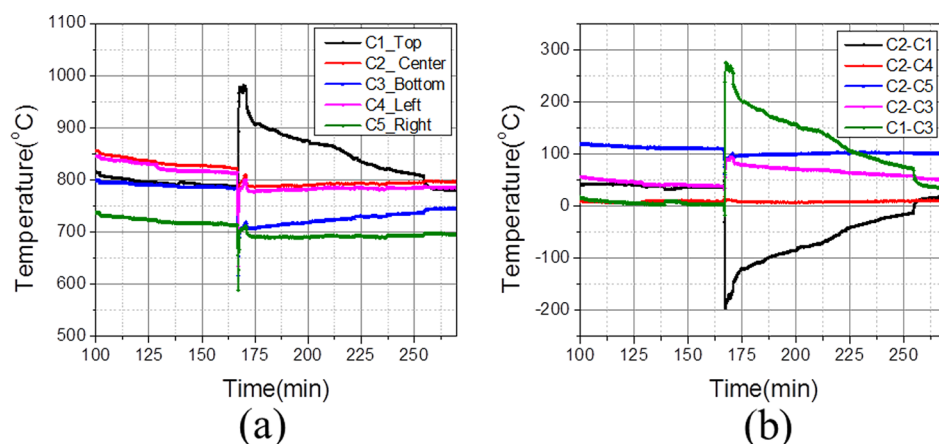


Figure 12. (a) Temperature distribution in the catalytic bed during the reaction with an emissivity value of 0.737. (b) Differences in temperature values at different locations of the catalytic bed with an emissivity value of 0.737.

flowing through the bed. Now, due to the sudden interruption of microwave energy input, reactant conversions were decreased and the concentration levels of H_2 , CO , CO_2 , and CH_4 changed in the catalytic bed after 30 s. Therefore, in this complex gas mixture environment, the dielectric properties of the whole catalytic bed changed. The second reason was that when MW power was switched on again, the catalyst was already at a temperature of ~ 600 °C, and so its dielectric properties were higher than at room temperature, resulting in a different response to absorb MW.

3.8. Axial and Radial Temperature Distribution during the Reaction. Figure 12a shows temperature values at the center, left, right, top, and bottom positions extracted after thermal data post processing. If a corrected emissivity is provided to the thermal camera, then temperature measurements in a 2D fashion will provide insight into the temperature distribution and heating patterns.

Figure 10b shows the locations at which the temperature data have been extracted from the thermal video of the reaction run. It is particularly interesting to map the axial and radial temperature distributions that occurred during the reaction run. Figure 12a shows the stable temperature differences at different points of the catalytic bed before the MW off issue and the clear shift, or separation, of temperature differences after MW on after 30 s of time gap. Figure 12b shows the differences in temperature in the mentioned location. In the case of a stable temperature before 166 min, the center and left point difference is 5–10 °C. The center-top and center-bottom temperature differences are in the range of 50–60 °C. The center-right temperature difference is ~ 120 °C, as the hot spot is on the left side only; hence there is significant temperature difference between the center and right positions. After 166 min, the hot zone shifts to the top part of the catalytic bed and influences the temperature distribution inside the catalytic bed. In this case, a clear separation of temperature differences is observed in Figure 12b. The -180 °C difference around 167 min shows that now the top part of the catalytic bed is hotter than the center part, which was indicated by the thermocouple reading and clearly shown in the thermal image (Figure 10c).

After this change in location of the hot spot, the top-center difference became 180 °C. The center-left temperature difference became ~ 10 –15 °C. The center-right temperature difference decreased from 120 to 100 °C, and the center-bottom one increased to 80–90 °C. A very big difference of

~ 280 °C from top to bottom after 167 min was observed. This top-bottom temperature difference decreased with an increase in time and eventually became ~ 50 °C at the end of 300 min.

CONCLUSIONS

The thermal camera–thermocouple dual temperature measurement method developed in this work allows for real-time high temperature (300–1000 °C) measurements in MW-heated catalytic reactors. This method was applied for a temperature distribution study in a platinum-on-carbon catalytic bed used for methane dry reforming. For this purpose, a custom-designed microwave cavity was employed to focus the microwave field on the catalyst bed and monitor its temperature in a 2D fashion by means of a thermal camera. The effect of different factors affecting the temperature measurements and emissivity values under microwave heating was investigated. The effects of camera range, the presence of different media and reactant gases in the process domain, object-to-camera distance, heating system, and microwave field distribution were discussed in detail. The multiparameter emissivity dependence in such a complex reaction system does not ensure correct temperature recording by the thermal camera alone; therefore, at least one contact sensor is highly recommended. The developed method successfully detected hot spot generation and provided an explanation for the nonhomogeneous heating profiles during MW processing. Careful handling and continued temperature monitoring with a thermal camera is very helpful to avoid potential risk hazards in MW-heated catalytic reactors.

ASSOCIATED CONTENT

Supporting Information

The Supporting Information is available free of charge on the ACS Publications website at DOI: 10.1021/acs.iecr.7b02091.

Effect of gases on emissivity under microwave heating; thermocouple and optical fiber temperature measurement comparison; emissivity measurement in conventional heating: (a) set up arrangement, (b) thermocouple at the center of catalytic bed, and (c) thermal image for emissivity calculation; reduction of sample volume in the second (a) and third cycle (b); challenges in reproducibility and risk factors involved: (a) fresh catalyst loaded in the microwave cavity; the black colored catalyst is visible through the transparent quartz

tube wall, (b) quartz tube after 15 h of heating and reaction experiments under MW heating, (c) white and black colored solid layer formed on the inside of the quartz tube wall, (d) thermal image showing the quartz tube breakage (PDF)

AUTHOR INFORMATION

Corresponding Authors

*E-mail: a.i.stankiewicz@tudelft.nl.

*E-mail: georgios.stefanidis@cit.kuleuven.be.

ORCID

Andrzej I. Stankiewicz: 0000-0002-8227-9660

Georgios D. Stefanidis: 0000-0002-4347-1350

Notes

The authors declare no competing financial interest.

ACKNOWLEDGMENTS

The research leading to these results has received funding from the European Research Council under the European Union's Seventh Framework Programme (FP7/2007-2013)/ERC grant agreement no. 267348.

REFERENCES

- Osepchuk, J. M. A History of Microwave Heating Applications. *IEEE Trans. Microwave Theory Tech.* **1984**, *32* (9), 1200.
- Sun, J.; Wang, W.; Yue, Q.; Ma, C.; Zhang, J.; Zhao, X.; Song, Z. Review on Microwave-Metal Discharges and Their Applications in Energy and Industrial Processes. *Appl. Energy* **2016**, *175*, 141.
- Stefanidis, G. D.; Muñoz, A. N.; Sturm, G. S. J.; Stankiewicz, A. A Helicopter View of Microwave Application to Chemical Processes: Reactions, Separations, and Equipment Concepts. *Rev. Chem. Eng.* **2014**, *30* (3), 1.
- Wang, Y.; Dai, L.; Fan, L.; Shan, S.; Liu, Y.; Ruan, R. Journal of Analytical and Applied Pyrolysis Review of Microwave-Assisted Lignin Conversion for Renewable Fuels and Chemicals. *J. Anal. Appl. Pyrolysis* **2016**, *119*, 104.
- Pang, Y.; Lei, H. Degradation of P-Nitrophenol through Microwave-Assisted Heterogeneous Activation of Peroxymonosulfate by Manganese Ferrite. *Chem. Eng. J.* **2016**, *287*, 585.
- Omran, M.; Fabritius, T.; Mattila, R. Thermally Assisted Liberation of High Phosphorus Oolitic Iron Ore: A Comparison between Microwave and Conventional Furnaces. *Powder Technol.* **2015**, *269*, 7.
- Oghbaei, M.; Mirzaee, O. Microwave versus Conventional Sintering: A Review of Fundamentals, Advantages and Applications. *J. Alloys Compd.* **2010**, *494* (1–2), 175.
- Acevedo, L.; Usón, S.; Uche, J. Exergy Transfer Analysis of Microwave Heating Systems. *Energy* **2014**, *68*, 349.
- Acevedo, L.; Usón, S.; Uche, J. Numerical Study of Cullet Glass Subjected to Microwave Heating and SiC Susceptor Effects. Part II: Exergy Transfer Analysis. *Energy Convers. Manage.* **2015**, *97*, 458.
- Chandrasekaran, S.; Ramanathan, S.; Basak, T. Microwave Material Processing — A Review. *AIChE J.* **2012**, *58* (2), 330–363.
- Goyette, J.; Chahine, R.; Bose, T. K.; Akyel, C.; Bosisio, R. Importance of the Dielectric Properties of Materials for Microwave Heating. *Drying Technol.* **1990**, *8* (5), 1111.
- Sturm, G. S. J.; Verweij, M. D.; Stankiewicz, A. I.; Stefanidis, G. D. Microwaves and Microreactors: Design Challenges and Remedies. *Chem. Eng. J.* **2014**, *243*, 147.
- Horikoshi, S.; Osawa, A.; Abe, M.; Serpone, N. On the Generation of Hot-Spots by Microwave Electric and Magnetic Fields and Their Impact on a Microwave-Assisted Heterogeneous Reaction in the Presence of Metallic Pd Nanoparticles on an Activated Carbon Support. *J. Phys. Chem. C* **2011**, *115* (46), 23030.
- Zhang, X.; Hayward, D. O.; Lee, C.; Mingos, D. M. P. Microwave Assisted Catalytic Reduction of Sulfur Dioxide with Methane over MoS₂ Catalysts. *Appl. Catal., B* **2001**, *33* (2), 137.
- Kappe, C. O. How to Measure Reaction Temperature in Microwave-Heated Transformations. *Chem. Soc. Rev.* **2013**, *42* (42), 4977.
- Durka, T.; Stefanidis, G.; Van Gerven, T.; Stankiewicz, A. On the Accuracy and Reproducibility of Fiber Optic (FO) and Infrared (IR) Temperature Measurements of Solid Materials in Microwave Applications. *Meas. Sci. Technol.* **2010**, *21* (4), 45108.
- Durka, T.; Stefanidis, G. D.; Van Gerven, T.; Stankiewicz, A. I. Microwave-Activated Methanol Steam Reforming for Hydrogen Production. *Int. J. Hydrogen Energy* **2011**, *36* (20), 12843.
- Ramirez, A.; Hueso, J. L.; Mallada, R.; Santamaria, J. In situ temperature measurements in microwave-heated gas-solid catalytic systems. Detection of hot spots and solid-fluid temperature gradients in the ethylene epoxidation reaction. *Chem. Eng. J.* **2017**, *316*, 50–60.
- Ramirez, A.; Hueso, J. L.; Mallada, R.; Santamaria, J. Ethylene Epoxidation in Microwave Heated Structured Reactors. *Catal. Today* **2016**, *273*, 99.
- Pert, E.; Carmel, Y.; Birnboim, A.; Olorunoyemi, T.; Gershon, D.; Calame, J.; Lloyd, I. K.; Wilson, O. C. Temperature Measurements during Microwave Processing: The Significance of Thermocouple Effects. *J. Am. Ceram. Soc.* **2001**, *84* (9), 1981.
- Will, H.; Scholz, P.; Ondruschka, B. Heterogeneous Gas-Phase Catalysis under Microwave Irradiation - A New Multi-Mode Microwave Applicator. *Top. Catal.* **2004**, *29* (3–4), 175.
- Li, L.; Jiang, X.; Wang, H.; Wang, J.; Song, Z.; Zhao, X.; Ma, C. Methane Dry and Mixed Reforming on the Mixture of Bio-Char and Nickel-Based Catalyst with Microwave Assistance. *J. Anal. Appl. Pyrolysis* **2017**, *125*, 318.
- Sturm, G. S. J.; Van Braam Houckgeest, A. Q.; Verweij, M. D.; Van Gerven, T.; Stankiewicz, A. I.; Stefanidis, G. D. Exploration of Rectangular Waveguides as a Basis for Microwave Enhanced Continuous Flow Chemistries. *Chem. Eng. Sci.* **2013**, *89*, 196.
- Luo, S. D.; Yang, Y. F.; Schaffer, G. B.; Qian, M. Calibration of Temperature Measurement by Infrared Pyrometry in Microwave Heating of Powder Materials: An Exothermic Reaction Based Approach **2013**, *47* (1), 5.
- Shen, X.; Xu, G.; Shao, C.; Cheng, C. Temperature Dependence of Infrared Emissivity of Doped Manganese Oxides in Different Wavebands (3–5 and 8–14 μm). *J. Alloys Compd.* **2009**, *479* (1), 420.
- Madding, R. P. Emissivity Measurement and Temperature Correction Accuracy Considerations. *Proc. SPIE* **1999**, *3700*, 393.
- Petrov, V. A.; Reznik, V. Y. Measurement of the Emissivity of Quartz Glass. *High Temp. - High Pressures* **1972**, *4*, 687–693.
- Catalá-Civera, J. M.; Canós, A. J.; Plaza-González, P.; Gutiérrez, J. D.; García-Bañós, B.; Peñaranda-Foix, F. L. Dynamic Measurement of Dielectric Properties of Materials at High Temperature during Microwave Heating in a Dual Mode Cylindrical Cavity. *IEEE Trans. Microwave Theory Tech.* **2015**, *63* (9), 2905.
- Peñaranda-Foix, F. L.; Janezic, M. D.; Catalá-Civera, J. M.; Canos, A. J. Full-Wave Analysis of Dielectric-Loaded Cylindrical Waveguides and Cavities Using a New Four-Port Ring Network. *IEEE Trans. Microwave Theory Tech.* **2012**, *60* (9), 2730.
- Chen, W.-H.; Liou, H.-J.; Hung, C.-I. A Numerical Approach of Interaction of Methane Thermocatalytic Decomposition and Microwave Irradiation. *Int. J. Hydrogen Energy* **2013**, *38* (30), 13260.
- Zhang, X.; Lee, C. S.; Mingos, D. M. P.; Hayward, D. O. Carbon Dioxide Reforming of Methane with Pt Catalysts Using Microwave Dielectric Heating. *Catal. Lett.* **2003**, *88* (June), 129.
- Fernandez, Y.; Fidalgo, B.; Pis, J. J.; Menendez, J. A.; Dominguez, J. Biogas to Syngas by Microwave-Assisted Dry Reforming in the Presence of Char. *Energy Fuels* **2007**, *21*, 2066.
- Fidalgo, B.; Dominguez, J.; Pis, J.; Menendez, J. Microwave-Assisted Dry Reforming of Methane. *Int. J. Hydrogen Energy* **2008**, *33* (16), 4337.